J|A|C|S
ARTICLES

Published on Web 02/04/2009

Multidimensional Exploration of Valley−Ridge Inflection Points on Potential-Energy Surfaces

April N. Sheppard and Orlando Acevedo*

Department of Chemistry and Biochemistry, Auburn University, Auburn, Alabama 36849

Received May 23, 2008; E-mail: orlando.acevedo@auburn.edu

Abstract: The ene reaction between singlet oxygen ($^1O_2$) and simple alkenes has been reported as the first experimentally supported example of a potential-energy surface (PES) featuring a valley−ridge inflection that contributes to the selectivity of product formation (*J. Am. Chem. Soc.* **2003**, *125*, 1319−1328). That PES, based on gas-phase ab initio calculations and experimental kinetic isotope effects, has shaped the current $^1O_2$ ene mechanism by advocating a concerted "two-step no-intermediate" mechanism. Our current investigation of the ene reaction between $^1O_2$ and tetramethylethylene in water, DMSO, and cyclohexane using novel 3-dimensional potentials of mean force (3-D PMF) calculations coupled to QM/MM simulations predicts an alternative free-energy surface that supports a traditional stepwise mechanism interpretation featuring a symmetric charge-separated perepoxide intermediate. Solvent polarity dictates the stability of the intermediate and controls the activation barrier for ene product formation. Transformation of the higher order condensed-phase 3-D PMF potential-energy surface, computed following three simultaneous reaction coordinates, into a downgraded 2-D surface results in the "two-step no-intermediate" mechanism. CCSD(T) and MP4(SDQ) free-energy maps in DMSO, constructed from a 3-D grid of B3LYP geometries using the CPCM solvent model, reproduce the QM/MM results and confirm that when solvent is taken into account the gas-phase bifurcation reaction pathway converts into a stepwise mechanism. This manuscript provides new insight into the biologically and synthetically important $^1O_2$ ene reaction and highlights a new multidimensional approach for constructing potential-energy surfaces.

Introduction

To begin the process of understanding chemical reactivity and selectivity for a specific system, it is typically useful to build a conceptual model of the potential-energy surface (PES). Briefly, the PES describes how the potential energy of a molecular system varies with structural change. For a large molecule, the corresponding PES has a high dimensionality resulting from a large number of degrees of freedom and as a consequence cannot be plotted nor visualized. However, a PES can be constructed through the structural variation of a few degrees of freedom within the molecular system to create a map of the energetic response. From a chemical viewpoint, the region of interest may follow one or two coordinates corresponding to the forming/breaking bonds of a specific reaction. For example, the ene reaction between singlet oxygen ($^1O_2$) and simple alkenes has recently been reported as the first experimentally supported example of a PES featuring a valley−ridge inflection (VRI) that is responsible for the selectivity of product formation.[1−3] In that work the PES was computed using two bond-making coordinates between the attacking oxygen of the $^1O_2$ and the olefinic carbons. Figure 1 gives a qualitative example of such a PES, where two transition states are connected as sequential saddle points on a three-dimensional potential-energy surface.

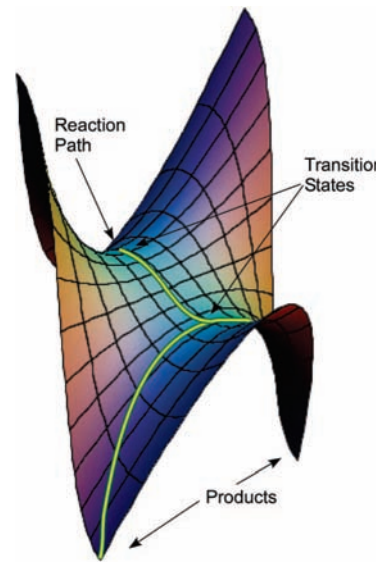

Figure 1. Qualitative potential-energy surface featuring a valley−ridge inflection.[4]

The $^1O_2$ ene reaction has attracted a great deal of interest due to its synthetic utility,[5] intriguing regiochemistry,[6] and biological significance.[7] However, determination of the mechanism between $^1O_2$ and monoolefins to form allylic hydroperoxides has proven to be highly challenging, particularly for theoretical methods.[8] While multiple concerted[1−3,9] and stepwise[10,11] pathways have been computationally predicted,

(1) Singleton, D. A.; Hang, C.; Szymanski, M. J.; Meyer, M. P.; Leach, A. G.; Kuwata, K. T.; Chen, J. S.; Greer, A.; Foote, C. S.; Houk, K. N. *J. Am. Chem. Soc.* **2003**, *125*, 1319–1328.
(2) Singleton, D. A.; Hang, C.; Szymanski, M. J.; Greenwald, E. E. *J. Am. Chem. Soc.* **2003**, *125*, 1176–1177.
(3) Leach, A. G.; Houk, K. N. *Chem. Commun.* **2002**, 1243–1255.

10.1021/ja803879k CCC: $40.75

Scheme 1. Traditional Ene Reaction Mechanism for the Ene Reaction between $^1O_2$ and Tetramethylethylene Featuring a (**1**) Rate-Limiting Transition State, (**2**) Perepoxide, and (**3**) Diradical or Zwitterionic Intermediate

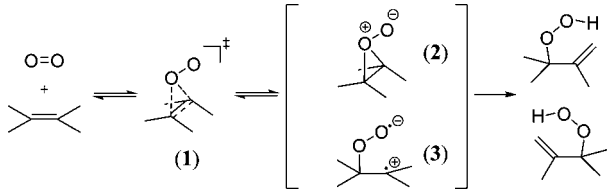

Scheme 2. "Two-Step No-Intermediate" Mechanism for the Ene Reaction between $^1O_2$ and Tetramethylethylene (where **2** is a perepoxide transition state)

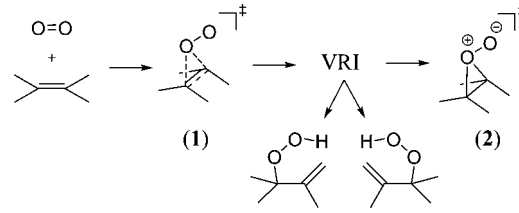

kinetic isotope effect (KIE) experiments[5,12−17] have traditionally been interpreted in terms of a stepwise mechanism where addition of $^1O_2$ to the alkene (**1**) is rate limiting and directly forms a perepoxide intermediate (**2**) that subsequently produces the ene products (Scheme 1). The participation of an open zwitterionic/biradical intermediate (**3**) in the reaction, while prevalent in theoretical studies,[10,11] has been effectively ruled out based on the absence of Markovnikov directing effects[13] and hypersensitive cyclopropyl probes designed to distinguish any open biradical or dipolar character for the intermediate in multiple solvents.[16]

More recently, a combined computational and experimental investigation by Singleton, Houk, Foote et al. suggested that for acyclic alkenes capable of undergoing the ene reaction, no intermediate exists at all.[1] In their proposed "two-step no-intermediate" mechanism, the symmetrical addition of $^1O_2$ was reported to be rate limiting on a PES that bifurcates at a VRI into two isomeric products prior to formation of a perepoxide-like transition structure (Scheme 2). The PES was constructed from gas-phase energy minimizations at the B3LYP/6-31G(d) theory level using a 2-D grid composed from the two C−O distances. Energies were determined from CCSD(T)/6-31G(d) single-point calculations on the B3LYP-optimized geometries.[1] The reported PES gave a shape similar to Figure 1. The inherent dangers of defining VRI points using a limited number of reaction coordinates have been reported in the literature by several groups including Baker,[18] Bosh,[19] Dive,[20] Schlegel,[21] Valtazanos,[22] and Wales.[23] In the case of the $^1O_2$ ene reaction, Singleton et al. provided significant validation of their potential-energy surface from multiple theory levels to following minimum energy paths using mass-weighted coordinates.[1] Such care must always be undertaken as composite grid searches are frequently prone to errors stemming from energy minimizations that do not reflect the effects of temperature or entropy and neglect of solvent effects, particularly important for a reaction featuring a developing charge separation.

Part of the difficulty of obtaining theoretical results consistent with experimental observations for the $^1O_2$ ene mechanism may stem from neglect of solvent effects in the calculations. Previous studies have found that while the rate of the $^1O_2$ ene reaction shows a negligible dependence on solvent polarity, product distribution can be substantially affected.[15,24] In addition, recent experimental observations of the enophile phenyl-1,2,4-triazoline-3,5-dione (PTAD) reacting with cyclopropyl-substituted alkenes[25] and our computational study of PTAD reacting with tetramethylethylene[26] in multiple solvents has provided evidence of large mechanistic changes significantly dependent on the reaction medium. Because of the similarities between the $^1O_2$ and triazolinedione ene reactions,[13,27] solvent may also play a considerable role in the mechanism of singlet oxygen.

Besides solvent effects, however, the largest introduction of error into the calculations may stem from a truncated description of the free-energy surface. To elucidate the effect of solvent on the $^1O_2$ ene mechanism and delineate its corresponding PES, the reaction between $^1O_2$ and tetramethylethylene has been investigated using multidimensional mixed quantum and molecular mechanics (QM/MM) simulations in three different explicit solvents: water, DMSO, and cyclohexane. Potential-energy surfaces were constructed using free-energy perturbation (FEP) calculations, but the surfaces were different from those previously calculated because they involved three simultaneous reaction coordinates: the two bonds that form between the attacking oxygen and both olefinic carbons, as used in the previous calculation,[1] and also the bond forming between the allylic hydrogen and the terminal oxygen. Activation barriers

(4) Palais, R. S.; Karcher, H. *3D-Xplor Math*, version 10.5; University of California: Irvine, CA, 2007.
(5) (a) Clennan, E. L. *Tetrahedron* **2000**, *56*, 9151–9179. (b) Clennan, E. L.; Pace, A. *Tetrahedron* **2005**, *61*, 6665–6691.
(6) Stratakis, M.; Orfanopoulos, M. *Tetrahedron* **2000**, *56*, 1595–1615.
(7) Greer, A. *Acc. Chem. Res.* **2006**, *39*, 797–804.
(8) Paterson, M. J.; Christiansen, O.; Jensen, F.; Ogilby, P. R. *Photochem. Photobiol.* **2006**, *82*, 1136–1160.
(9) (a) Houk, K. N.; Williams, J. C., Jr.; Mitchell, P. A.; Yamaguchi, K. *J. Am. Chem. Soc.* **1981**, *103*, 949–951. (b) Gonzalez-Lafont, A.; Moreno, M.; Lluch, J. M. *J. Am. Chem. Soc.* **2004**, *126*, 13089–13094.
(10) Harding, L. B.; Goddard, W. A., III *J. Am. Chem. Soc.* **1980**, *102*, 439–449.
(11) (a) Yamaguchi, K.; Yabushita, S.; Fueno, T.; Houk, K. N. *J. Am. Chem. Soc.* **1981**, *103*, 5043–5046. (b) Tonachini, G.; Schlegel, H. B.; Bernardi, F.; Robb, M. A. *J. Am. Chem. Soc.* **1990**, *112*, 483–491. (c) Sevin, F.; McKee, M. L. *J. Am. Chem. Soc.* **2001**, *123*, 4591–4600. (d) Maranzana, A.; Canepa, C.; Ghigo, G.; Tonachini, G. *Eur. J. Org. Chem.* **2005**, 3643–3649.
(12) Stephenson, L. M.; Grdina, M. J.; Orfanopoulos, M. *Acc. Chem. Res.* **1980**, *13*, 419–425.
(13) Orfanopoulos, M.; Smonou, I.; Foote, C. S. *J. Am. Chem. Soc.* **1990**, *112*, 3607–3614.
(14) Poon, T. H. W.; Pringle, K.; Foote, C. S. *J. Am. Chem. Soc.* **1995**, *117*, 7611–7618.
(15) Alberti, M. N.; Orfanopoulos, M. *Tetrahedron* **2006**, *62*, 10660–10675.
(16) Alberti, M. N.; Orfanopoulos, M. *Org. Lett.* **2008**, *10*, 2465–2568.
(17) Alberti, M. N.; Vassilikogiannakis, G.; Orfanopoulos, M. *Org. Lett.* **2008**, *10*, 3997–4000.
(18) Baker, J.; Gill, P. M. W. *J. Comput. Chem.* **1988**, *9*, 465–475.
(19) Bosch, E.; Moreno, M.; Lluch, J. M.; Bertrán, J. *Chem. Phys. Lett.* **1989**, *160*, 543–548.
(20) Ramquet, M.-N.; Dive, G.; Dehareng, D. *J. Chem. Phys.* **2000**, *112*, 4923–4934.
(21) Schlegel, H. B. *J. Chem. Soc., Faraday Trans.* **1994**, *90*, 1569–1574.
(22) Valtazanos, P.; Ruedenberg, K. *Theor. Chim. Acta* **1986**, *69*, 281–307.
(23) Wales, D. J. *J. Chem. Phys.* **2000**, *113*, 3926–3927.
(24) Lissi, E. A.; Encinas, M. V.; Lemp, E.; Rubio, M. A. *Chem. Rev.* **1993**, *93*, 699–723.
(25) Roubelakis, M. M.; Vougioukalakis, G. C.; Angelis, Y. S.; Orfanopoulos, M. *Org. Lett.* **2006**, *8*, 39–42.
(26) Acevedo, O.; Squillacote, M. E. *J. Org. Chem.* **2008**, *73*, 912–922.
(27) Orfanopoulos, M.; Stratakis, M.; Elemes, Y. *Tetrahedron Lett.* **1989**, *30*, 4875–4878.

were computed with complete sampling of the geometry for the reacting systems and explicit interactions with solvent molecules.

The simulations provide evidence of a new PES that corresponds to a traditional stepwise mechanistic interpretation featuring an intermediate with the symmetry of a perepoxide.[28] This alternative PES also finds the initial addition of $^1O_2$ to tetramethylethylene to be rate limiting, as expected from kinetic isotope effect observations, with calculated free energies in good agreement with experimental measurements. However, a perepoxide ground-state intermediate is predicted to form in a stepwise fashion prior to formation of the ene products, in opposition to the "two-step no-intermediate" mechanism. The simulations find that solvent polarity dictates the stability of the charge-separated perepoxide intermediate and controls the magnitude of the activation barrier for ene product formation. Degradation of the multiple condensed-phase free-energy surfaces required to construct the 3-D QM/MM/FEP PES into a 2-D surface based on the two reaction coordinates used by Singleton et al.[1] yields the "two-step no-intermediate" mechanism. High-level ab initio calculations at the CCSD(T) and MP4(SDQ) theory levels using the CPCM solvent model confirm the QM/MM/FEP results. This manuscript provides new insight into the $^1O_2$ ene reaction and highlights a new multidimensional approach for constructing potential-energy surfaces for similar reactions.

Computational Methods

The present study explores the effect of solvent and PES dimensionality on the ene reaction between $^1O_2$ and tetramethylethylene using mixed quantum and molecular mechanics (QM/MM) simulations.[29] Reactants, intermediates, transition states, and products were located in water, DMSO, and cyclohexane solvents with the reacting system treated using the PDDG/PM3 semiempirical molecular orbital method;[30] semiempirical calculations have played a significant role in establishing the mechanism of molecular oxygen transitions.[8,31] PDDG/PM3 has given excellent results for a wide variety of organic and enzymatic reactions in solution-phase QM/MM studies,[32,33] including the ene reaction.[26] The solvent molecules are represented explicitly using the TIP4P water model,[34] the united-atom OPLS force field for DMSO,[35] and an all-atom OPLS force field for cyclohexane.[36] BOSS 4.6[37] was used to carry out the reaction in stored solvent boxes with the exception of cyclohexane, which was custom-made in a similar fashion to previous liquid simulations of alkanes.[38] The resulting cyclohexane box exhibited both a density (0.76 g/mL) and a heat of vaporization (33.0 kJ/mol) at 25 °C that corresponded to experimental data for liquid cyclohexane (density, 0.7785 g/mL;[39] heat of vaporization, 33.334 kJ/mol).[40]

In the current QM/MM methodology, the systems consisted of the reactants plus 395 solvent molecules for DMSO and cyclohexane or 740 water molecules. The boxes are periodic and tetragonal with $c/a = 1.5$, where a is 25, 31, and 36 Å for water, DMSO, and cyclohexane, respectively. The solute's intramolecular energy is treated quantum mechanically using PDDG/PM3; computation of the QM energy and atomic charges is performed for each attempted move of the solute, which occurred every 100 configurations. For electrostatic contributions to the solute−solvent energy CM3 charges[41] were obtained for the solute with a scaling factor of 1.14. In addition, Lennard−Jones interactions between solute and solvent atoms were taken into account using OPLS parameters. This combination is appropriate for a PM3-based method as it minimizes errors in computed free energies of hydration.[42] Solute−solvent and solvent−solvent intermolecular cutoff distances of 12 Å were employed. Quadratic feathering of the intermolecular interactions within 0.5 Å of the cutoff was applied to soften the energy discontinuity. Changes in free energy were calculated using free-energy perturbation (FEP) theory in conjunction with NPT Metropolis Monte Carlo (MC) simulations at 25 °C and 1 atm. Total translations and rotations were sampled in ranges that led to overall acceptance rates of about 32−42% for new configurations in water and DMSO and about 15% in cyclohexane. Multiple FEP windows were run simultaneously on a Linux cluster located at Auburn University.

CCSD(T) and MP4(SDQ) single-point calculations on a 3-D grid of B3LYP-optimized[43] geometries were also used to construct potential-energy surfaces in vacuum and DMSO using Gaussian 03.[44] The 6-31G(d) basis set was used in all cases. The effect of solvent was explored by full DFT geometry optimizations using the conductor-like polarizable continuum model (CPCM)[45] with the UFF cavity model; a dielectric constant of 46.7 was used for DMSO. Subsequent ab initio single-point calculations were also carried out using the CPCM model. All ab initio and DFT calculations were carried out on computers located at the Alabama Supercomputer Center.

Results and Discussion

PES from 2 Reaction Coordinates. To explore the adequacy of using two reaction coordinates to construct a potential-energy surface for the $^1O_2$ ene reaction it is necessary to consider which coordinates are the most appropriate to follow. Singleton et al. incrementally fixed the lengths of the two forming C−O bonds in conjugation with B3LYP/6-31G(d) optimizations on all other variables to construct a 15 × 15 grid of the reaction surface.[1] However, it is important to take into account that an allylic hydrogen is abstracted via the terminal oxygen at some stage of the reaction pathway, and it would be advantageous to control

(28) Grdina, S. B.; Orfanopoulos, M.; Stephenson, L. M. *J. Am. Chem. Soc.* **1979**, *101*, 3111–3112.
(29) (a) Aqvist, J.; Warshel, A *Chem. Rev.* **1993**, *93*, 2523–2544. (b) Gao, J. *Acc. Chem. Res.* **1996**, *29*, 298–305. (c) Kaminski, G. A.; Jorgensen, W. L. *J. Phys. Chem. B* **1998**, *102*, 1787–1796.
(30) Repasky, M. P.; Chandrasekhar, J.; Jorgensen, W. L. *J. Comput. Chem.* **2002**, *23*, 1601–1622.
(31) Minaev, B. F. *Int. J. Quantum Chem.* **1980**, *17*, 367–374.
(32) (a) Acevedo, O.; Jorgensen, W. L. *Org. Lett.* **2004**, *6*, 2881–2884. (b) Acevedo, O.; Jorgensen, W. L. *J. Am. Chem. Soc.* **2005**, *127*, 8829–8834. (c) Acevedo, O.; Jorgensen, W. L. *J. Am. Chem. Soc.* **2006**, *128*, 6141–6146. (d) Acevedo, O.; Jorgensen, W. L. *J. Org. Chem.* **2006**, *71*, 4896–4902. (e) Acevedo, O.; Jorgensen, W. L. *J. Chem. Theory Comput.* **2007**, *3*, 1412–1419. (f) Acevedo, O.; Jorgensen, W. L.; Evanseck, J. D. *J. Chem. Theory Comput.* **2007**, *3*, 132–138.
(33) Tubert-Brohman, I.; Acevedo, O.; Jorgensen, W. L. *J. Am. Chem. Soc.* **2006**, *128*, 16904–16913.
(34) Jorgensen, W. L.; Chandrasekhar, J.; Madura, J. D.; Impey, W.; Klein, M. L. *J. Chem. Phys.* **1983**, *79*, 926–935.
(35) Jorgensen, W. L.; Briggs, J. M.; Contreras, M. L. *J. Phys. Chem.* **1990**, *94*, 1683–1686.
(36) Jorgensen, W. L.; Maxwell, D. S.; Tirado-Rives, J. *J. Am. Chem. Soc.* **1996**, *118*, 11225–11236.
(37) Jorgensen, W. L.; Tirado-Rives, J. *J. Comput. Chem.* **2005**, *26*, 1689–1700.
(38) Thomas, L. L.; Christakis, T. J.; Jorgensen, W. L. *J. Phys. Chem. B* **2006**, *110*, 21198–21204.
(39) *CRC Handbook of Chemistry and Physics*, 68th ed.; CRC Press, Inc.: Boca Raton, FL, 1987−1988; p C-224.
(40) Aston, J. G.; Szasz, G. J.; Fink, H. L. *J. Am. Chem. Soc.* **1943**, *65*, 1135–1139.
(41) Thompson, J. D.; Cramer, C. J.; Truhlar, D. G. *J. Comput. Chem.* **2003**, *24*, 1291–1304.
(42) Udier-Blagovic, M.; De Tirado, P. M.; Pearlman, S. A.; Jorgensen, W. L. *J. Comput. Chem.* **2004**, *25*, 1322–1332.
(43) (a) Becke, A. D. *J. Chem. Phys.* **1993**, *98*, 5648–5652. (b) Lee, C.; Yang, W.; Parr, R. G. *Phys. Rev.* **1988**, *37*, 785–789.
(44) Frisch, M. J. *Gaussian 03*, Revision D.01; Gaussian, Inc.: Wallingford, CT, 2004 [Full reference given in the Supporting Information].
(45) Cossi, M.; Rega, N.; Scalmani, G.; Barone, V. *J. Comput. Chem.* **2003**, *24*, 669–681.

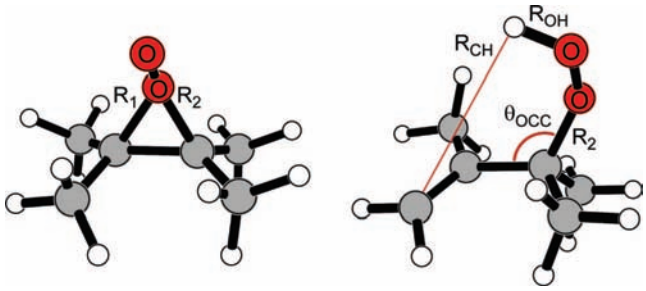

Figure 2. Reaction coordinates R_1 and R_2 (free-energy map 1) and R_{OH} and θ_{OCC} (free-energy map 2) for the ene reaction between singlet oxygen and tetramethylethylene. Illustrated structures are the perepoxide and product from aqueous-phase QM/MM/MC simulations.

the hydrogen transfer as a coordinate as well. In a similar fashion to our previous work on the triazolinedione ene reaction,[26] two separate 2-dimensional potentials of mean force (PMF) free-energy maps were constructed in solution by perturbing the lengths of the two forming C−O bonds, R_1 and R_2, for the first free-energy map (similar to Singleton et al.)[1] and the bond angle, θ_{OCC}, with a hydrogen abstraction coordinate, R_{OH}, for the second map (Figure 2). It was necessary to use multiple gas-phase-optimized structures to provide good starting points for the reaction profile in the MC/FEP free-energy maps. Six different starting structures per map were chosen, one for approximately every 0.4 Å or 25° bond and angle perturbations. Starting structures were optimized near the medial configuration of the range. All internal degrees of freedom, minus the reaction coordinates, were fully sampled during the simulations. Each FEP calculation involved 5 million configurations of equilibration and 10 million configurations of averaging and was computed using distance and angle-bending increments of 0.05 Å and 0.5°, respectively.

The resultant free-energy maps for the reaction in DMSO are shown in Figure 3 and required 86−126 million single-point QM calculations each (maps in water and cyclohexane are given in the Supporting Information as Figures S1 and S2). Figure 3A details the reaction between $^1O_2$ and tetramethylethylene using a maximum $R_1 = R_2$ separation of ca. 2.55 Å (final energy calculations begin from a 10 Å separation, as discussed in the Energetics section). The symmetrical addition of $^1O_2$ to tetramethylethylene was found to be the rate-limiting transition structure, TS_{add}, as expected, but intriguingly a charge-separated perepoxide intermediate was also located. Free-energy map 1 should be comparable to the PES predicted by Singleton et al. as the same reaction coordinates were used; however, the results are considerably different, e.g., no appreciable hydrogen transfer has occurred and the perepoxide is a ground-state intermediate as opposed to a transition state. Free-energy map 2 (Figure 3B) also located the identical ground-state perepoxide (within the level of uncertainty in the results, ca. ±0.02 Å after refinement) using the R_{OH} and θ_{OCC} reaction coordinates in ranges of 0.95−2.30 Å and 57.5−130°. In addition, free-energy map 2 found the ene product and a transition structure, TS_{abs}, separating the perepoxide from the product. Upon initial inspection of the MC/FEP calculations, the free-energy maps appear to be consistent with a stepwise mechanism with two transition structures and a perepoxide intermediate, as opposed to the "two-step no-intermediate" mechanism.

Given that the present 2-D PESs are considerably different from the reported PES featuring a valley−ridge inflection and no intermediate[1,3] many different starting configurations were used to ensure no bias was introduced into our calculations.

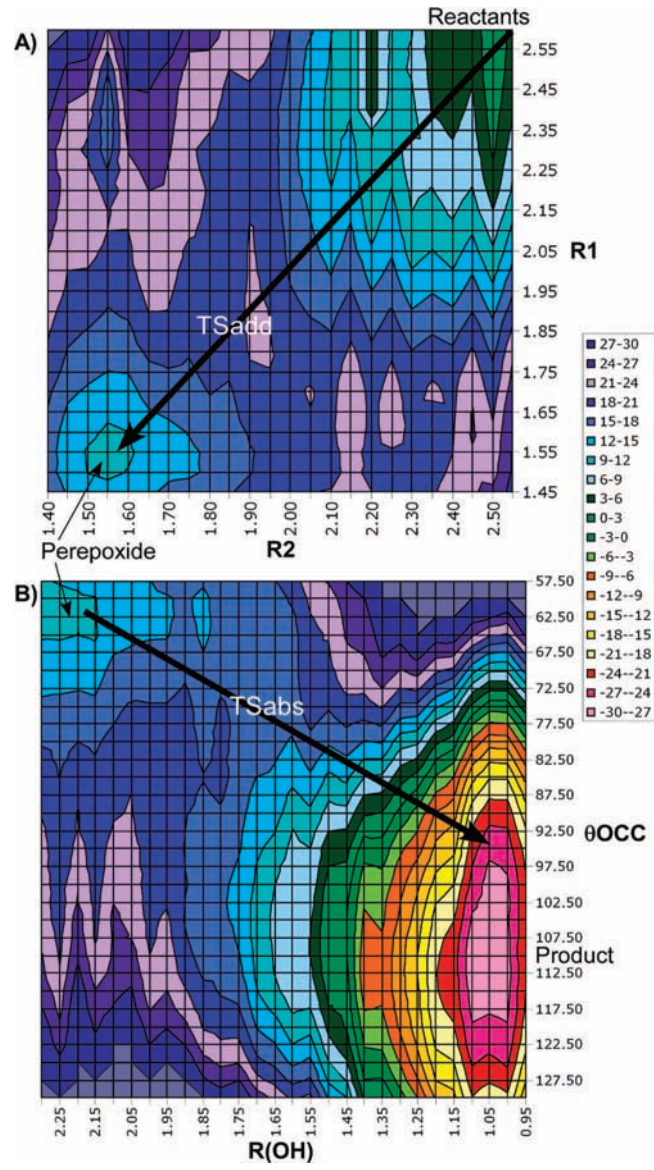

Figure 3. Two-dimensional potentials of mean force (free-energy maps) for the ene reaction in DMSO. (A) Free-energy map 1: arrow follows path from reactants through TS_{add} to the perepoxide. (B) Free-energy map 2: arrow follows route from the perepoxide through TS_{abs} to product. All distances in angstroms, angles in degrees, and relative free-energy in kcal/mol. Energy value range truncated from −30 to 30 kcal/mol on figure for clarity.

Regardless of the initial geometries used to start the simulations, the computed PES surface was unchanged. Another possible reason for the deviation between PESs may come from the choice of reaction coordinates in conjunction with the starting structures. For example, beginning the simulations with the allylic hydrogen chemically bonded to carbon in free-energy map 1 may have prevented R_{OH} from reaching a distance necessary for hydrogen transfer to the terminal oxygen to occur as R_1 and R_2 were perturbed. While the present calculations included extensive sampling of the substrates and hundreds of solvent molecules to obtain configurationally averaged free-energy changes, inadequate sampling of any of the reaction coordinates could have led to a higher noise level in the Monte Carlo simulations. Hence, to adequately traverse the free-energy surface beginning from the rate-limiting transition state toward product it is necessary to control three reaction coordinates, R_1,

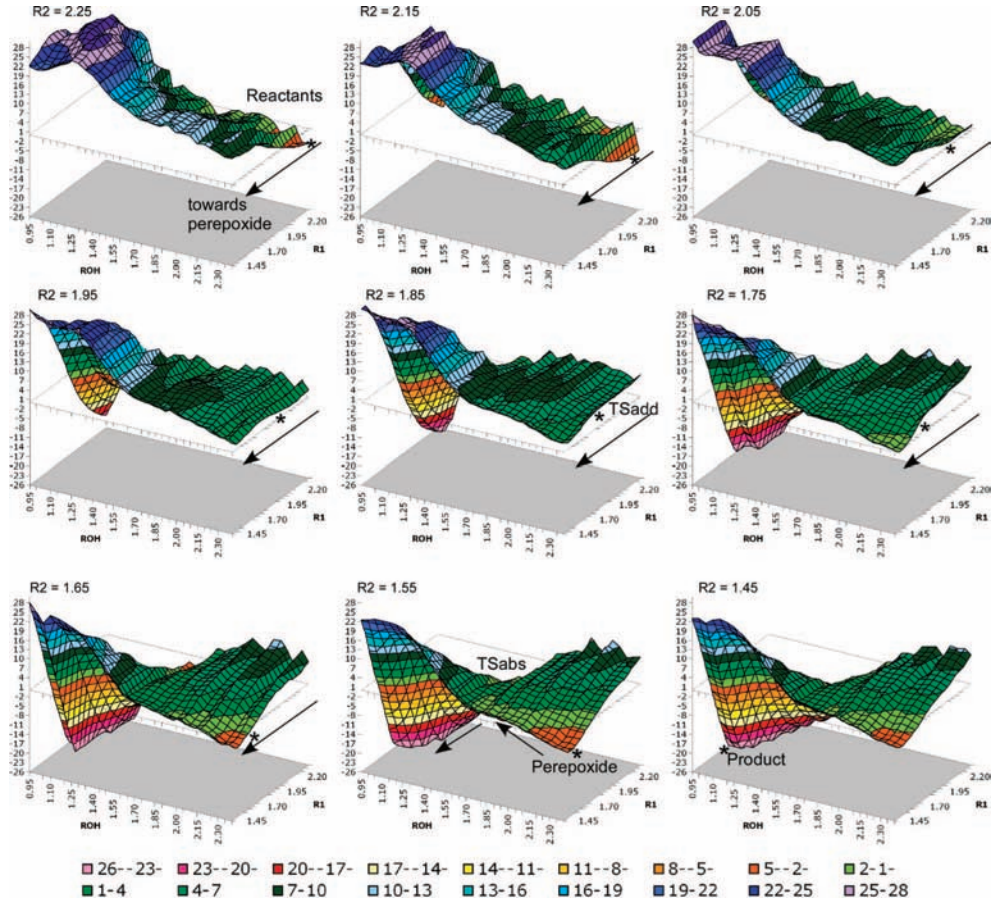

Figure 4. Three-dimensional potentials of mean force (free-energy maps) for the ene reaction in DMSO. Multiple free-energy maps are required to visualize three simultaneous reaction coordinates, R_1, R_2, and R_{OH}. Each individual map represents a PES slice where R_2 is fixed at a certain value (1.45−2.25 Å) with R_1 and R_{OH} distances given on the *X* and *Y* axes. The arrow and asterisk follow the minimum energy path from reactants through TS_{add} to perepoxide then finally over TS_{abs} to give the product. All distances in angstroms and relative free-energy (given on the *Z* axis) in kcal/mol. Energy value range truncated from −26 to 28 kcal/mol on figure for clarity.

R_2, and R_{OH}, simultaneously. The importance of using three reaction coordinates to map out energy surfaces has been reported by Valtazanos et al. for the ring opening of cyclopropylidene using early theoretical techniques.[46]

PES from 3 Reaction Coordinates. The question becomes how to carry out a simulation that follows three simultaneous reaction coordinates, considering the difficulty of conceptualizing a 4-dimensional result with energy included. A common approximation of simultaneous bond making and breaking can be used to reduce the dimensionality of the problem.[33,47] As an example, the attacking oxygen−carbon distances could have identical reaction coordinates, $R_1 = R_2$, with C_s symmetry leading toward the perepoxide. However, introducing a constraint in the potentials of mean force (PMF) calculations can result in an overestimation of the reaction barrier[33] or at worst give an incorrect description of the potential-energy surface. Instead, a new method is proposed, 3-D PMF, following the model of 3-D and 4-D NMR, where the 2-D spectrum is spread out over additional dimensions. In this method, nine separate free-energy maps were constructed with R_2 values held constant from 1.45 to 2.25 Å in increments of 0.1 Å while the reaction coordinates R_1 and R_{OH} were perturbed in 0.05 Å increments, as previously described. The nine individual maps were then combined into a single PES through normalization of the energies to the first map ($R_2 = 1.45$ Å) via FEP calculations by fixing R_{OH} and R_1 to 2.35 and 1.55 Å, respectively, while perturbing R_2 from 1.45 to 2.25 Å in increments of 0.05 Å. To our knowledge, this is the first report of FEP results for an organic reaction using three simultaneous reaction coordinates.

In order to visualize the PES, Figure 4 gives the 3-D PMF as nine individual slices of the total PES represented sequentially by fixed R_2 distances beginning from 2.25 Å and decreasing toward 1.45 Å. The minimum free-energy path is shown by an arrow and asterisks in Figure 4 as $^1O_2$ approaches the alkene. The 3-D PMF results predict a stepwise mechanism in DMSO once again; following the rate-limiting transition structure, TS_{add} (see $R_2 = 1.85$ Å slice in Figure 4), the perepoxide is formed directly as an intermediate and a second activation barrier, TS_{abs}, must be overcome prior to formation of product (see $R_2 = 1.55$ Å slice in Figure 4). The 3-D PMF PESs were also computed for water and cyclohexane and gave similar results (given in the Supporting Information as Figures S3 and S4).

Transformation of the PES from 3-D to 2-D. Assuming the 3-D PMF results are correct, why does a 15 × 15 composite grid using ab initio and density functional theory calculations produce a PES featuring a valley−ridge inflection and a perepoxide transition state?[1] The neglect of solvent effects, temperature, and entropy likely make the most significant

(46) Valtazanos, P.; Elbert, S. T.; Ruedenberg, K. *J. Am. Chem. Soc.* **1986**, *108*, 3147–3149.
(47) Gao, J.; Ma, S.; Major, D. T.; Nam, K.; Pu, J.; Truhlar, D. G. *Chem. Rev.* **2006**, *106*, 3188–3209.

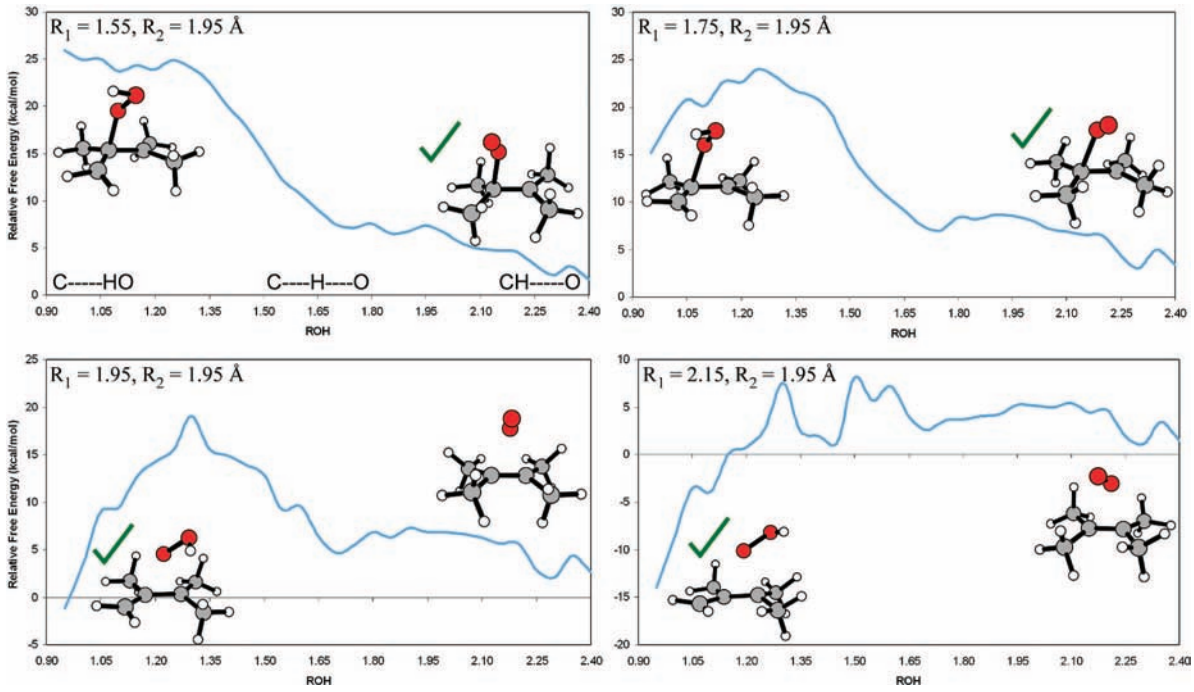

Figure 5. Representative slices of the potential-energy surface (R_1 = 1.55, 1.75, 1.95, and 2.15 Å) where R_2 is fixed at 1.95 Å and R_{OH} is varied from 0.95 to 2.40 Å. On each slice the ene solute has two possible minima, where the allylic hydrogen is bonded to either the terminal oxygen or carbon atom. A green checkmark indicates the energetically favored conformer.

contributions to the reported PES description. However, a second possibility for the deviation could come from the selection and number of reaction coordinates used. Whereas the R_1 and R_2 distances are fixed throughout the optimization, the remaining geometries, including the R_{OH} distance, are completely dependent on the minimization algorithm used in the composite grid search. In other words, energy minimization algorithms, such as those available in the Gaussian 03 program[44] and used to compute the 2-D $^1O_2$ ene PES,[1,3] are designed to search for the lowest energy conformation and, barring user error, will always produce either a local or a global minimum. From chemical intuition this means that for any combination of R_1 and R_2 selected, R_{OH} can only realistically exist in one of two value ranges: a short R_{OH} (ca. 0.95 Å) where the hydrogen is chemically bonded to the terminal oxygen or a long R_{OH} (ca. 2.40 Å) where the hydrogen is bonded to the allylic carbon. No other conformations are possible as the resultant energy would always be higher.

As proof of concept, Figure 5 takes the 3-D PMF potential-energy surface slice where R_2 is fixed at 1.95 Å (see Figure 4) and further slices the map at R_1 = 1.55, 1.75, 1.95, and 2.15 Å. The result is four static R_1 and R_2 distance data points (e.g., R_1 = 1.55 and R_2 = 1.95 Å in the first slice, R_1 = 1.75 and R_2 = 1.95 Å in the second slice, etc.), exactly like the composite grid method reported by Singleton et al.[1] However, unlike the 2-D grid method which reports only the energy minimization for each R_1 and R_2 combination, the 3-D PMF calculations can also explicitly follow the energy path required to transfer the allylic hydrogen from the carbon to the terminal oxygen as a function of distance between the H and O atoms at any given combination of R_1 and R_2 values. In every case the lowest energy configurations will have the hydrogen covalently bonded to either a C or O atom (as indicated by the green checkmark in Figure 5). Accordingly, optimization of each grid point using density functional theory will only result in geometries and energies

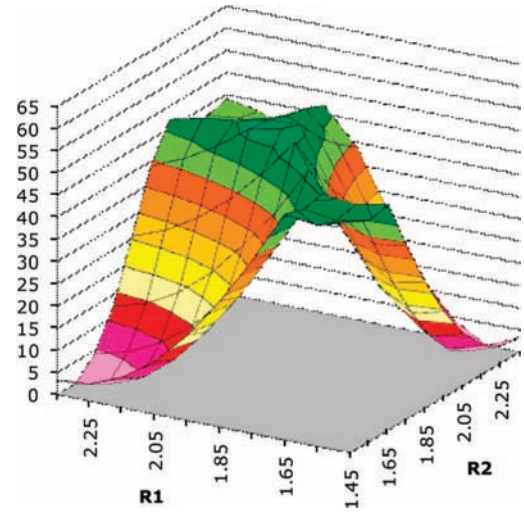

Figure 6. Transformation of the three-dimensional potentials of mean force (free-energy map) in cyclohexane into a two-dimensional free-energy map based on two reaction coordinates, R_1 and R_2. The minimum energy value for R_{OH} was chosen for every unique R_1 and R_2 combination. All distances in angstroms and relative free-energy in kcal/mol.

consistent with the minimum energy value for R_{OH} for every unique R_1 and R_2 combination.

By examining only the energy minima for each R_1 and R_2 pair from the nine QM/MM/FEP free-energy maps (Figure 4) the 3-D PES can be downgraded into a 2-D surface. The results were plotted for the ene reaction and given as Figure 6. Immediately it is clear that the resultant PES closely resembles Figure 1 and the grid-based 2-D PES for the $^1O_2$ ene reaction. A valley−ridge inflection is predicted to occur, and the perepoxide is no longer an intermediate but a transition state connecting the products! Kinetic isotope effects (KIE) computed on a 2-D free energy surface for the rate-limiting grid saddle point should reproduce experiment well because the transition

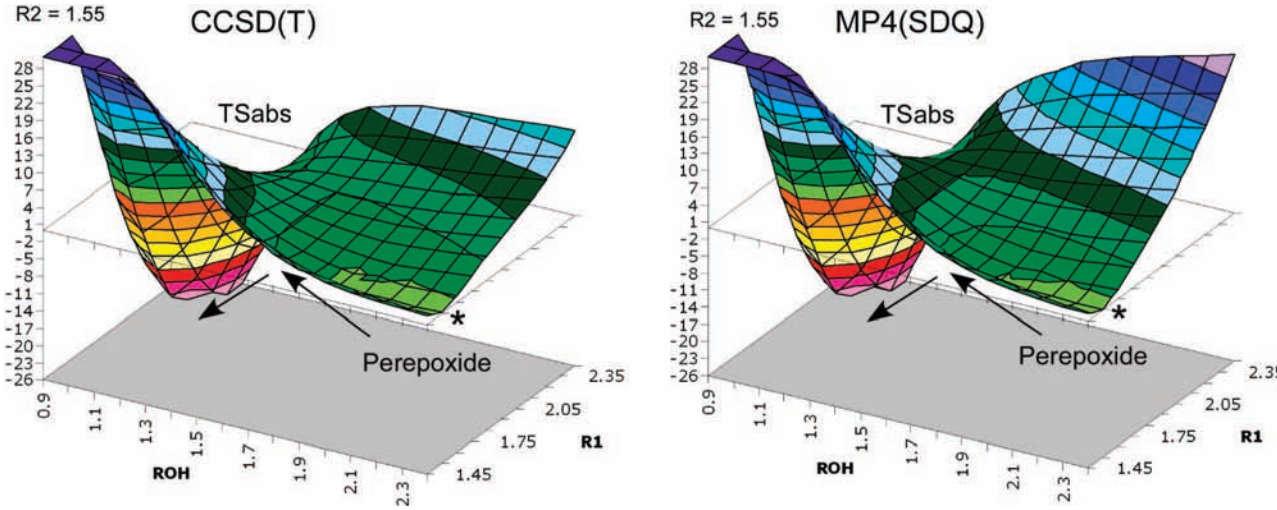

Figure 7. CCSD(T)/6-31G(d) and MP4(SDQ)/6-31G(d) single-point energy maps in DMSO for the ene reaction between $^1O_2$ and tetramethylethylene optimized using B3LYP/6-31G(d) and CPCM. These individual maps represent a PES slice where R_2 is fixed at 1.55 Å with R_1 and R_{OH} distances given on the *X* and *Y* axes. The arrow and asterisk follow the minimum energy path from perepoxide through TS_{abs} to give the product. All distances in angstroms and relative free-energy (given on the *Z* axis) in kcal/mol. Energy value range truncated from −26 to 28 kcal/mol on figure for clarity.

structure is identical to TS_{add} on the 3-D PMF PES. The calculated KIE for TS_{add} reported by Singleton et al. is within experimental error,[1] which was given as support of the accuracy for the remaining portion of the CCSD(T)/B3LYP-derived PES. The higher-order 3-D PMF calculations now show this assumption may not be justified. However, it is important to note that the current results are for the solution-phase ene reaction, and the mechanism may still follow the "two-step no-intermediate" pathway in the gas phase.

Ab Initio Calculations. The semiempirical PDDG/PM3 closed-shell method's ability to accurately describe the singlet oxygen's open-shell electronic structure is certainly a concern to be addressed; hence, high-level ab initio calculations were carried out to validate the QM/MM results. The same methodology presented in the Singleton et al. paper,[1] i.e., CCSD(T)/6-31G(d) single-point energy calculations on a 16 × 11 grid of B3LYP/6-31G(d)-optimized geometries, was used. However, in our case a 3-D grid was employed following the format of the QM/MM/FEP calculations where R_2 was exclusively fixed at 1.55 Å while R_1 and R_{OH} were incrementally fixed from 1.45 to 2.45 Å and 0.90 to 2.35 Å, respectively, in units of 0.5 Å; the remaining variables were fully optimized. In addition, a DMSO solvent environment was approximated by energy minimizing the structures using DFT in combination with the CPCM continuum solvation model and subsequently computing CCSD(T) single points in CPCM as well. The resultant energy surface for the CCSD(T)//B3LYP/CPCM singlet oxygen ene reaction is given in Figure 7 and is strikingly similar to the R_2 = 1.55 Å slice from Figure 4 obtained using the PDDG/PM3/MM/FEP calculations. Additional figures for B3LYP-, CCSD(T)-, and MP4(SDQ)-derived potential-energy maps in the gas phase and in DMSO solution are given in the Supporting Information.

The initial DFT gas-phase potential-energy surface predicts no barrier for formation of product, which is not unexpected as B3LYP calculations have been reported to proceed without an energy barrier for the attack of $^1O_2$ on tetramethylethylene.[1] Singleton et al. determined the only transition state that could be located at the restricted DFT theory level was the C_s-symmetric perepoxide with an activation barrier of −14.0 kcal/mol.[1] However, our gas-phase single-point calculations using CCSD(T) and MP4(SDQ) on the DFT-derived geometries predict an intermediate prior to formation of the product (see the Supporting Information for the energy maps). The MP4(SDQ) method gives the perepoxide as the intermediate with an energy barrier of 2.1 kcal/mol, and CCSD(T) finds an open intermediate with an activation barrier of 13.3 kcal/mol toward product. As previous experimental evidence has ruled out the existence of an open intermediate,[16] the use of two reaction coordinates instead of three to map out the gas-phase PES may be appropriate at the CCSD(T) theory level. However, the inclusion of solvent into the calculations brings all results into alignment, switching the "two-step no-intermediate" reaction pathway into a stepwise mechanism featuring the perepoxide as the sole intermediate prior to formation of product. B3LYP predicts a shallow barrier of 0.6 kcal/mol between perepoxide and product, but CCSD(T) and MP4(SDQ) predict more substantial energy barriers of 4.2 and 7.3 kcal/mol, which is in good agreement with the computed PDDG/PM3 barrier in DMSO, $\Delta G^{\ddagger} = 7.0$ kcal/mol. Further comparisons between the computed geometries and energies using the ab initio and semiempirical methods are given below.

Structures. To locate the critical points of the reaction more precisely, the regions surrounding the free-energy minima and maxima from the 3-D PMF free-energy maps (i.e., TS_{add}, perepoxide, TS_{abs}, and product) were refined with increments of 0.01 Å and 0.05°, accordingly. The PDDG/PM3 geometries of the refined structures in each of the three solvents are listed in Table 1. The rate-determining transition state, TS_{add}, had making/breaking bond distances of ca. 1.84 Å in DMSO and cyclohexane, but water had an earlier transition state at ca. 1.94 Å. Previously reported gas-phase calculations for TS_{add} using the HF, B3LYP, UB3LYP, and CASSCF methods with the 6-31G(d) basis set gave values for R_1 and R_2 of 1.93 and 1.93, 1.67 and 1.67, 2.42 and 1.84, 2.40 and 1.89 Å, respectively.[1] The reported 2D CCSD(T)/6-31G(d)//B3LYP/6-31G(d) grid predicted a much earlier transition state with symmetrical R_1 and R_2 distances of 2.38 Å.[1] A recent reinvestigation of the reaction using a 2-D CASMP2/6-31G(d)//UB3LYP/6-31G(d) grid gave symmetrical R_1 and R_2 distances of 2.04 Å; constrained optimizations at CASMP2/6-31G(d) for the symmetrical C−O distances showed the highest energy point between 2.1 and 2.2 Å.[48]

Table 1. Computed Bond Lengths (Å) and Angles (deg) for the Ene Reaction Structures Between $^1O_2$ and Tetramethylethylene at 25 °C and 1 atm[a]

	R_1	R_2	R_{OH}	R_{CH}	θ_{OCC}
water					
TS_{add}	1.94	1.93	2.60	1.05	68.9
perepoxide	1.50	1.53	2.48	1.11	60.0
TS_{abs}	1.76	1.52	1.69	1.23	71.9
product	2.45	1.47	1.00	4.10	112.0
DMSO					
TS_{add}	1.85	1.84	2.39	1.10	67.3
perepoxide	1.53	1.54	2.38	1.19	61.0
TS_{abs}	1.80	1.50	1.69	1.11	75.4
product	2.46	1.43	0.99	4.35	112.0
cyclohexane					
TS_{add}	1.84	1.81	2.54	1.10	66.9
perepoxide	1.54	1.55	2.47	1.13	61.0
TS_{abs}	1.80	1.55	1.72	1.15	73.3
product	2.47	1.47	0.95	4.40	111.0

[a] From the 3-D free-energy maps computed in the QM/MM/MC simulations.

The geometries for the transition structure leading to ene product via an allylic proton transfer, TS_{abs}, were found to have similar R_1 and R_2 distances in the three solvents. The TS_{abs} geometries computed using the CCSD(T) and MP4(SDQ) methods in DMSO are similar to the PDDG/PM3 values with the exception that R_1 is longer with a value of ca. 2.05 Å, but the R_{OH} value of 1.60 Å compares well to the 1.69 Å from the QM/MM simulations. It must be kept in mind however that the geometries were derived from a B3LYP-optimized grid. For a better comparison, the TS_{abs} structure was optimized using MP2/6-31+G(d) in CPCM DMSO solvent and in the gas phase; a single imaginary frequency confirmed a true transition structure via a frequency calculation. The MP2-optimized TS_{abs} geometries of $R_1 = 1.96$ Å, $R_2 = 1.56$ Å, $R_{OH} = 1.55$, $R_{CH} = 1.21$ Å, and $\theta_{OCC} = 80.4°$ agree favorably with the QM/MM/FEP geometries in DMSO (see Table 1). Intramolecular kinetic isotope effects (KIE) were computed for the gas-phase MP2 TS_{abs} structure using the QUIVER program[49] from theoretical vibrational frequencies scaled by 0.9427[50] in conjunction with methodology from Bigeleisen and Mayer.[51] No tunneling corrections were made for the hydrogen-abstraction reaction as the accuracy of the simple correction has been reported as questionable.[1] The ^2H KIE was computed to be 1.278 at 25 °C (exptl. value = 1.38−1.41 in acetone-d_6 at −10 °C)[28] and the olefinic ^{13}C and reacting methyl ^{13}C KIEs were computed as 0.945 (exptl. value = 1.011(4) and 1.008(1))[1] and 0.933 (exptl. value = 1.009(6) and 1.009(3)),[1] respectively. The computed results for the gas-phase-optimized structure are reasonably close to experimental values, particularly when compared to the recent solvent-independent measurement of $k_H/k_D = 1.20 \pm 0.5$ at 0 °C for the proton abstraction step between singlet oxygen and (*S,S*)-*cis*-1,4-diphenyl-2-butene-1,4-d_2, which was reported to proceed via a perepoxide intermediate.[17]

The degree of bond breaking between the carbon and allylic hydrogen is more advanced in water with a R_{CH} distance of 1.23 Å compared to 1.11 and 1.15 Å in DMSO and cyclohexane, respectively. The later transition structure in water is consistent with the larger activation barrier computed for product formation relative to the aprotic solvents. Stabilization of the charge-separated intermediate is the major factor dictating geometry changes, and its relationship with respect to energy and charges is discussed below.

Table 2. Free Energy Changes, ΔG (kcal/mol), at 25 °C for the Ene Reaction between $^1O_2$ and Tetramethylethylene Using QM/MM/MC[a]

	water	DMSO	cyclohexane
reactants	0	0	0
TS_{add}	13.5	10.4	12.5
perepoxide	−4.3	1.8	5.0
TS_{abs}	4.5	8.8	11.4
product	−23.2	−46.3	−54.0

[a] Experimental $\Delta G^‡$ (kcal/mol) for TS_{add} = ca. 8.8 kcal/mol in cyclohexane.

Energetics. Activation barriers were computed for the ene reaction in solution beginning from a 10 Å separation distance for $^1O_2$ and tetramethylethylene. This distance was chosen to ensure an adequate separation between the reactants and avoid any possible stabilization from an exciplex complex, i.e., the free-energy surfaces were flat in this vicinity. New simulation boxes of a significantly larger size were required in order to avoid energetic artifacts stemming from the 12 Å cutoff distance exceeding one-half the distance of the minimum image convention. The new boxes constructed were periodic and cubic, where each side is 40, 61, and 54 Å for water, DMSO, and cyclohexane, respectively, with 2239, 1986, and 852 solvent molecules. Monte Carlo sampling was increased to 20 million configurations of equilibration and averaging per 0.02 Å double-wide FEP window. The ΔG values predicted from the QM/MM/MC simulations in the larger boxes are summarized in Table 2 and account for a 1 M standard state via a cratic correction of 1.89 kcal/mol.[52] Error ranges in the calculated free-energy values have been estimated from fluctuations in the ΔG values for each FEP window using the batch means procedure with batch sizes of 0.5 M configurations.[37] Statistical uncertainties for the free-energy of activation ($\Delta G^‡$) in TS_{add} were computed as 0.4, 0.4, and 0.5 kcal/mol in water, DMSO, and cyclohexane, respectively, while those found for the free-energy of the reaction (ΔG_{rxn}) were 0.5 kcal/mol for all solvents computed.

The $\Delta G^‡$ values predicted from the QM/MM/MC simulations for TS_{add} are 13.5, 10.4, and 12.5 kcal/mol in water, DMSO, and cyclohexane. The experimental $\Delta G^‡$ is 8.2 kcal/mol in both toluene[53] and CS_2;[54] correcting for the known rate change upon going from toluene to cyclohexane ($k(C_6H_5CH_3)/k(C_6H_{12}) = 2.67$)[24] allows us to derive a $\Delta G^‡$ value of ca. 8.8 kcal/mol for the present reaction in cyclohexane. The calculated activation barriers are in reasonable agreement with experimental data and reproduce well the rate differences between the solvents. A gas-phase PDDG/PM3 $\Delta G^‡$ value of 26.3 kcal/mol was computed when the two reactants were brought together in a C_s-symmetric fashion, $R_1 = R_2$, in increments of 0.05 Å using FEP theory and Monte Carlo sampling (see Supporting Information Figure S9). The computed barrier is overestimated from a predicted experimental range of 10.1−15.1 based on the reported gas-

(48) Leach, A. G.; Houk, K. N.; Foote, C. S. *J. Org. Chem.* **2008**, *73*, 8511–8519.
(49) Saunders, M.; Laidig, K. E.; Wolfsberg, M. *J. Am. Chem. Soc.* **1989**, *111*, 8989–8994.
(50) Scott, A. P.; Radom, L. *J. Phys. Chem.* **1996**, *100*, 16502.
(51) Bigeleisen, J.; Mayer, M. G. *J. Chem. Phys.* **1947**, *15*, 261–267.
(52) Yu, B. Y. *J. Pharm. Sci.* **2001**, *90*, 2099–2102.
(53) Gorman, A. A.; Hamblett, I.; Lambert, C.; Spencer, B.; Standen, M. C. *J. Am. Chem. Soc.* **1988**, *110*, 8053–8059.
(54) Hurst, J. R.; Schuster, G. B. *J. Am. Chem. Soc.* **1982**, *104*, 6854–6856.

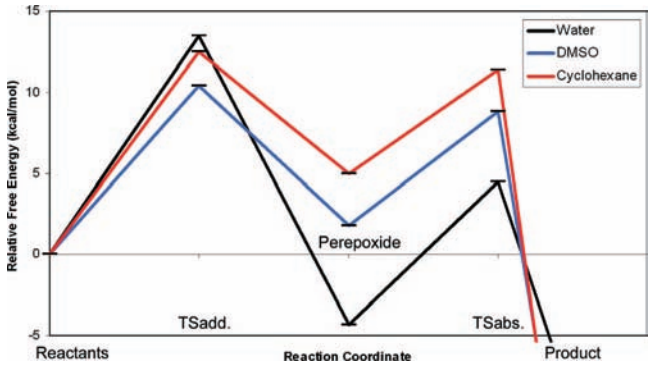

Figure 8. Free-energy profiles for the ene reaction between $^1O_2$ and tetramethylethylene in the three solvents from QM/MM/MC calculations. Energy values truncated to −5 kcal/mol on figure for clarity.

phase enthalpy value[55] and entropies from time-resolved techniques in CS_2.[56] Enforcing a C_s reaction pathway and additional entropy penalties for constraining the reactants to be within a sphere of 4.5 Å certainly raised the computed energy of the gas-phase reaction. However, the condensed-phase cyclohexane QM/MM calculations without such limitations also overestimated experimental values by ca. 3.7 kcal/mol.

Addition of $^1O_2$ was found to be energetically rate limiting in all solvents and the reaction subsequently proceeded directly to a perepoxide intermediate with ΔG values of −4.3, 1.8, and 5.0 kcal/mol in water, DMSO, and cyclohexane relative to reactants. The importance of including solvent effects in the calculations is evident as gas-phase CASSCF theoretical calculations predicted that the energy of the perepoxide lies 14.8 kcal/mol above the reactants.[10] The charge separation present in the perepoxide intermediate is expected to be extremely sensitive to solvent polarity and hydrogen bonding, and accordingly, a direct correlation of increasing perepoxide stability with increasing solvent polarity (2.02, 46.7, and 78.4 debye for cyclohexane, DMSO, and water) was found (Figure 8). This appears to be consistent with early reports of trapping a perepoxide intermediate for the ene reaction between $^1O_2$ and tetramethylethylene in 40% aqueous acetone;[57] however, claims that the trapping experiment is invalid have been made.[58] Foote and co-workers also found that more polar solvents, CH_3CN versus CCl_4, eased the trapping of a perepoxide intermediate between $^1O_2$ and *trans*-cyclooctene.[14] A perepoxide was also reported to be trapped by phosphites in the reaction of adamalideneandamantane (Ad=Ad) with singlet oxygen in benezene.[59] More recently, however, Foote and co-workers reported difficulties when trying to trap a perepoxide with simple alkenes despite extensive efforts.[1]

The ene product forming transition structure, TS_{abs}, was also computed and gave $\Delta G^{\ddagger}$ values of 4.5, 8.8, and 11.4 kcal/mol in water, DMSO, and cyclohexane relative to reactants. Comparing the $\Delta\Delta G^{\ddagger}$ from the perepoxide to TS_{abs} yields relative energy barriers of 8.8, 7.0, and 6.4 kcal/mol in water, DMSO, and cyclohexane, i.e., increasing the polarity of the solvent increases this energy barrier for hydrogen abstraction. No experimental values have been reported for the activation barrier from perepoxide to product, but comparison of our 3-D grid energy values of 4.2 and 7.3 kcal/mol using the CCSD(T) and MP4(SDQ) single-point calculations, respectively, in DMSO suggest the QM/MM results are reasonable.

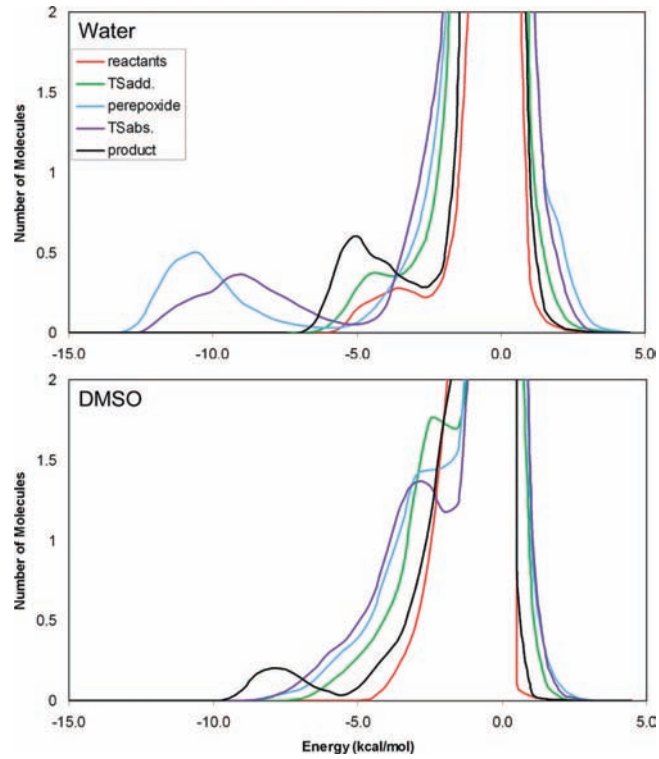

Figure 9. Solute−solvent energy pair distributions for the reaction between $^1O_2$ and tetramethylethylene in water and DMSO for the reactants, transition structures (TS_{add} and TS_{abs}), perepoxide intermediate, and the product. The ordinate records the number of solvent molecules that interact with the solutes with their interaction energy on the abscissa. Units for the ordinate are number of molecules per kcal/mol.

Solvation. Changes in solvation along the reaction pathways are available from the present QM/MM/MC calculations. In particular, the solute−solvent energy pair distributions record the average number of solvent molecules that interact with the solute and the associated energy. The interaction energies are quantified by analyzing the results in five representative windows, near the reactants, the perepoxide, the addition and product-forming transition states, and the product. The results for the ene reaction in water and DMSO are shown in Figure 9, and data for cyclohexane can be found in the Supporting Information. Hydrogen bonding in water and the most favorable electrostatic interactions in DMSO and cyclohexane are reflected in the left-most region with solute−solvent interaction energies more attractive than −5 kcal/mol. The large bands near 0 kcal/mol are a result of the many distant solvent molecules located in the outer shells.

In viewing Figures 9 and S5 (Supporting Information) it is immediately clear that the perepoxide intermediate and TS_{abs} have considerably stronger energy bands in aqueous solution compared to TS_{add} and the reactants. In addition, large differences are found between the energy pair distributions for the perepoxide and TS_{abs} in water compared to the aprotic solvents. The low-energy bands arise from hydrogen-bond donation to the terminal oxygen. Hydrogen bonding is known to be sensitive

(55) Ashford, R. D.; Ogryzlo, E. A. *J. Am. Chem. Soc.* **1975**, *97*, 3604–3607.
(56) Hurst, J. R.; Wilson, S. L.; Schuster, G. B. *Tetrahedron* **1985**, *41*, 2191–2197.
(57) Fenical, W.; Kearns, D. R.; Radlick, P. *J. Am. Chem. Soc.* **1969**, *91*, 7771–7772.
(58) Gollnick, K.; Haisch, D.; Schade, G. *J. Am. Chem. Soc.* **1972**, *94*, 1747–1748.
(59) Stratakis, M.; Orfanopoulos, M.; Foote, C. S. *Tetrahedron Lett.* **1991**, *32*, 863–866.

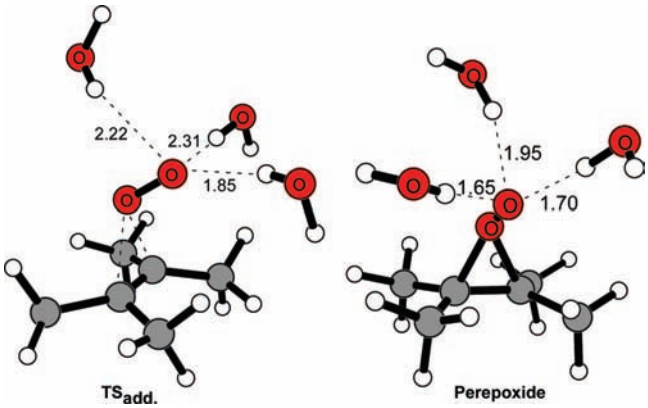

Figure 10. Typical snapshot for the rate-limiting transition structure, TS_{add}, and the perepoxide intermediate from the ene reaction between $^1O_2$ and tetramethylethylene in water (only nearest water molecules are illustrated). Distances in angstroms.

to small charge shifts, particularly in the ene reaction.[26] Hence, the low-energy bands centered around −11 kcal/mol for the perepoxide suggest a better stabilization of the strongly dipolar character of the attacking and terminal oxygen atoms in aqueous solution (+0.21, −0.64 e) compared to DMSO (+0.25, −0.61 e) and cyclohexane (+0.30, −0.59 e). The energy peak for TS_{abs}, ca. −9 kcal/mol in water, is slightly reduced compared to the intermediate; however, once again the magnitude of the O^+O^- charge separation is dictated by the solvent polarity with greater stabilization from hydrogen bonding in water (+0.11, −0.60 e), which is not possible in the aprotic solvents DMSO (+0.11, −0.57 e) and cyclohexane (+0.16, −0.52 e). The charge separation is significantly smaller for TS_{add} in all solvents with O^+O^- values of (+0.04, −0.31e) in water, (+0.11,−0.38 e) in DMSO, and (+0.08, −0.40 e) in cyclohexane. TS_{add} had similar energy band strengths in both water and DMSO (Figure 9), which is consistent with reported rates of reaction showing a negligible dependence on solvent polarity.

Integration of the energy bands from −15 to −4.5 kcal/mol yields 0.4 water molecules for the reactants, 0.8 for TS_{add}, 3.2 for the perepoxide, 3.0 for TS_{abs}, and 1.9 for the product. From the display of configurations such as in Figure 10, on average there are three short strong O···H hydrogen bonds from water molecules with the terminal oxygen of the perepoxide compared to the longer, weaker hydrogen bonds for the rate-limiting transition state. Integration of the bands for the TS_{add}, perepoxide, and TS_{abs} structures from −15.0 to −4.5 kcal/mol in DMSO yields 1.0, 1.8, and 2.2 solvent molecules, respectively, with a large shift toward weaker interaction energies when compared to water. The dipole interaction from the DMSO solvent is simply weaker and less specific than hydrogen bonding with water. Cyclohexane had no favorable interactions for any of the structures along the reaction pathway, which is consistent with a nonpolar aprotic solvent. The principal contributor to the stabilization of the perepoxide in the water clearly arises from enhanced interactions between the solvent molecules and the highly polarized oxygen atoms present in the intermediate.

The solute−solvent structure for the ene reaction in water can be further characterized by radial distribution functions, $g(R)$. Hydrogen bonding between the terminal oxygen of $^1O_2$ and the hydrogens of water, $O(^1O_2)$−H(water), should yield contacts shorter than 2.5 Å. The corresponding $g_{OH}(R)$ gives the probability of finding a hydrogen of water at a distance R from the terminal oxygen in the ene reaction. The $^1O_2$ ene reaction shows a well-defined first peak centered around 1.7 Å with a minima around 2.5 Å. The large magnitude of the peaks for the perepoxide and TS_{abs} reflects the significantly stronger hydrogen-bonding interactions occurring compared to the reduced peak for TS_{add} (Figure 11). Integration of the first peaks to the minima reveals averages of 3.0 hydrogen bonds between the terminal oxygen of the ene reaction and water molecules for the perepoxide, well illustrated in Figure 10, and yields 2.1 hydrogen bonds for TS_{add}. The snapshot of TS_{add} in Figure 10 indicates that the hydrogen bonds are a little longer on average, and the reduced interactions in TS_{add} are in good accord with the weaker energy bands found in the energy pair distributions. The overall picture supports the fact that hydrogen bonding is very sensitive to charge distributions, so the system is more affected by the progression from the perepoxide to TS_{abs} in water than in DMSO with its weaker ion−dipole interactions. Thus, the higher activation barrier for TS_{abs} relative to the perepoxide in water compared to DMSO and cyclohexane ($\Delta\Delta G$ = 8.8, 7.4, and 6.0 kcal/mol, respectively) results from the significant stabilization of hydrogen bonding with the charge-separated intermediate.

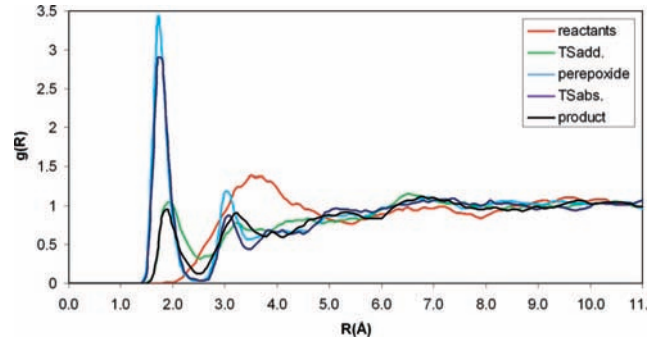

Figure 11. Computed terminal $O(^1O_2)$−H(water) radial distribution functions for the reaction between $^1O_2$ and tetramethylethylene at 25 °C.

Conclusions

The ene reaction between $^1O_2$ and tetramethylethylene has recently been reported as the first experimentally supported example of a PES featuring a valley−ridge inflection with significant chemical consequences for product selectivity.[1−3] That PES, constructed from the composite of CCSD(T) single-point energies on a grid of B3LYP geometries in the gas-phase, supported a reaction surface featuring two adjacent transition states without an intervening intermediate. However, the current solution-phase calculations using a novel three-dimensional (3-D) potentials of mean force method coupled to QM/MM simulations present an alternative PES which supports a traditional stepwise mechanism interpretation featuring a symmetric charge-separated perepoxide intermediate. By examining the energy minima from the 3-D PMF free-energy maps, the PES could be downgraded into a 2-D surface. The resultant solution-phase PES for the $^1O_2$ ene reaction closely resembled the previous gas-phase "two-step no-intermediate" mechanism. CCSD(T) and MP4(SDQ) potential-energy surface calculations, derived from a 3-D grid of B3LYP geometries optimized using the CPCM DMSO solvent model, reproduced the QM/MM/FEP free-energy surface with a perepoxide intermediate and an ene product-forming transition state present.

The current study has provided additional insight into the effect of solvent on the $^1O_2$ ene reaction through energy pair

distributions, radial distribution functions, and changes in charges along the reaction pathway. The most significant solvent effect reported is the change in the reaction pathway from the gas-phase "two-step no-intermediate" mechanism to a stepwise reaction. The charge separation present in the perepoxide intermediate is expected to be extremely sensitive to solvent polarity and hydrogen bonding; accordingly, a direct correlation of increasing perepoxide stability with increasing solvent polarity was found. In addition, increasing the polarity of the solvents was found to increase the relative energy barrier for product formation, solidifying the perepoxide's role as an intermediate and not a transition state in solution. The findings reported here may have a significant impact on other computationally derived PESs featuring a valley−ridge inflection.

Acknowledgment. Gratitude is expressed to Auburn University and the Alabama Supercomputer Center for support of this research. Discussions with Prof. Michael E. Squillacote are also appreciated.

Supporting Information Available: Free-energy maps from 2-D and 3-D PMF simulations and ab initio/DFT/CPCM calculations for the reaction in water, DMSO, and cyclohexane; additional solute−solvent energy pair distribution in cyclohexane; energies, frequencies, and coordinates of all structures computed using ab initio and DFT; KIE Quiver calculations; and complete ref 44. This material is available free of charge via the Internet at http://pubs.acs.org.

JA803879K